Korean J. Chem. Eng., 40(3), 618-629 (2023)
DOI: 10.1007/s11814-022-1337-3

pISSN: 0256-1115
eISSN: 1975-7220

The effect of cold atmospheric plasma (CAP) on the formation of reactive oxygen species and treatment of *Porphyromonas gingivalis* biofilm *in vitro* for application in treatment of peri-implantitis

Chang-Min Lee[*,‡], Young-IL Jeong[*,‡], Yun Kyong Lim[**], Joong-Ki Kook[**], Seong-Won Yang[***], Min-Suk Kook[**,†], and Byung-Hoon Kim[*,†]**

*Department of Dental Materials, College of Dentistry, Chosun University, Gwangju 61452, Korea
**Department of Oral Biochemistry, College of Dentistry, Chosun University, Gwangju 61452, Korea
***Department of Ophthalmology, College of Medicine, Chosun University, Gwangju 61452, Korea
****Department of Maxillofacial Surgery, School of Dentistry, Chonnam National University, Gwangju 61186, Korea
(*Received 13 July 2022 • Revised 25 October 2022 • Accepted 6 November 2022*)

Abstract−Cold atmospheric plasma (CAP) has been investigated to control local infections, such as peri-implantitis or periodontitis, since reactive oxygen species (ROS) and reactive nitrogen species (RNS) produced from CAP have excellent antibacterial activity. *Porphyromonas gingivalis* (*P. gingivalis*) grown on titanium (Ti) disks was treated with CAP under various conditions *in vitro* and assessed for its antibacterial capacity. CAP apparatus was designed to treat periodontitis. *P. gingivalis* biofilm was formed onto the Ti disks for application in periodontitis treatment. True power of plasma jet plume from CAP apparatus gradually increased according to increase of intensity/energy level ratio. Optical emission spectroscopy (OES) of plasma jet plume from CAP equipment showed that the peaks of Ar^+, OH and O^- ions were observed in the UV range (200 nm-400 nm) and visible range (690 nm-950 nm). In OES analysis, the peaks of OH and O^- ions were relatively increased when the volume of oxygen supply was decreased compared to Ar. Furthermore, the increase of plasma intensity increased the peaks of OH and O^- ions. *P. gingivalis* biofilm was formed onto the Ti disks and confirmed viability of *P. gingivalis*. Production of ROS in the aqueous solution by CAP apparatus gradually increased according to the treatment time and intensity of plasma. The increased ROS level induced decrease of surviving *P. gingivalis* according to treatment time and intensity of plasma. Furthermore, CAP treatment of *P. gingivalis* biofilm on the Ti disks also induced death of bacterial cells. Longer treatment time and higher energy level of CAP apparatus resulted in decrease of HGF-1 cell viability. Thus, appropriate treatment time and intensity of plasma is required to minimize cytotoxicity against normal cells with bactericidal effect. Practically, 6.387 W of plasma power and 60 s of treatment time was considered as an appropriate treatment condition to diminish normal cell cytotoxicity. We suggest that the CAP apparatus is a promising candidate to eradicate biofilm with antibacterial efficacy through ROS generation from CAP apparatus.

Keywords: Cold Atmospheric Plasma, Reactive Oxygen Species, Periodontitis, *P. gingivalis*, Antibacterial Activity

INTRODUCTION

Peri-implantitis, which is a severe infection and inflammatory process surrounding dental implants, frequently induces loss of bone and various health problems in the other organs [1-3]. Peri-implantitis affects dental implants, can destroy alveolar bone surrounding implantation, induces loss of dental implants and affects various systemic diseases [2]. Especially, pathogens in the gum and/or oral cavity form sticky film composed of bacteria and gradually build up hardened biofilm on the implant [3]. Biofilm on the implant, which induces peri-implantitis, is difficult to remove with normal brushing and/or flossing. For removal of biofilm in the implant and/or gum, a mechanical cleaning procedure is the typical treatment option currently. However, mechanical cleaning normally requires local anesthesia and is time-consuming [4,5]. Otherwise, systemic chemotherapy using antibiotics has delivery problems, i.e., antimicrobial agents have difficulties in the penetration to the therapeutic region into deep gingiva and induce drug resistance problem against treated antibiotics [5]. Matthes et al. reported that enzymes can be used to destabilize hardened biofilm on the implant surfaces with acceptable cell tolerability and then help to remove biofilm [4]. They argue that 2,500 μg/ml lysozyme affected hardening biofilm and destabilized 10%. Bone graft materials formulated with antibiotics for sustained prolonging in the local area provide healing of peri-implantitis lesions, i.e., released antibiotics from the bone graft material resulting in decontamination of implant surface and healing of soft/hard tissues [5]. However, these materials are required to be approved their extended durations of biocompatibility and essential biomaterial features for material longevity in the oral cavity.

Cold atmospheric plasma (CAP) has been extensively investigated in the field of antibacterial and anticancer therapy in last several decades [6-8]. Intrinsic properties of CAP in a biological system are to generate ROS and/or reactive nitrogen species (RNS) in the

†To whom correspondence should be addressed.
E-mail: omskook@jnu.ac.kr, kim5055@chosun.ac.kr
‡These authors equally contributed to this work.

system, and ROS/RNS in the biological system has antibacterial/anticancer activity [6-8]. Even though appropriate levels of ROS/RNS in the biological system are required to maintain cell proliferation and differentiation, excessive levels of ROS/RNS in the biological system typically induces oxidative stress against target cells or bacteria and then suppresses their growth [9-11]. Especially, CAP can be considered as an ideal device to treat periodontal disease with minimal side-effects against surrounding cells/tissues compared to systemic chemotherapy [11-16]. Plasma jet has been considered as an ideal candidate for treatment of periodontal disease in experimental models and clinical trials [13,14] For example, Kusakci-Seker et al. reported that non-thermal atmospheric plasma (NTP) has a protective effect on the loss of alveolar bone derived from periodontitis [14]. The plasma jet has effectiveness in suppression of planktonic growth and biofilm of *P. gingivalis* with cell safe manner [15]. The plasma jet has an inhibitory effect on the formation of biofilm on the zirconia surfaces [16]. Hong et al., suggested that ROS induced DNA damage of bacterial cells through oxidative stresses following with DNA breaks, membrane depolarization and cell death [17]. Vatansever also reported that ROS including hydrogen peroxide, hydroxyl radicals and singlet oxygen affects the antioxidant defense system against ROS in bacterial cells and then oxidative degradation of bacterial membrane following with death of bacterial cells [18]. Furthermore, Hong et al., reported that *P. gingivalis*-induced biofilm can be destroyed by ROS generated by plasma treatment through physicochemical damages against bacterial biofilms [19]. Then, ROS including various singlet oxygens is important to kill bacteria and destroy biofilm. Due to these intrinsic properties, CAP is considered as a safe treatment option for periodontal disease.

In this study we investigated the ROS producing capacity of CAP equipment and its antibacterial activity against *in vitro* peri-implantitis model. For *in vitro* peri-implantitis model, *P. gingivalis* was grown onto the Ti disks to make bacterial biofilm, and then biofilm was used to assess biological capacity of CAP equipment. Practically, Hong et al., also reported that argon (Ar) and oxygen-based cold plasma have efficacy in the removal of *P. gingivalis* biofilm and then induce death of bacteria [19]. However, they are not reporting the formation of ROS/RNS including hydrogen peroxide, singlet oxygens, hydroxyl radicals and nitric oxides. They must be specifically affecting the viability of bacteria in the biofilm and destruction of biofilm since principal roles of CAP are to generate various kind of ROS and RNS excessively in the biological system. These will control unwanted reactions abnormal cell or pathogen. Then, we focused on the ROS/RNS formation by Ar/oxygen-based CAP equipment since ROS-producing capacity of CAP is critical for antibacterial activity. The potential of CAP equipment on the ROS/RNS-producing capacity was assessed in the inhibition of *P. gingivalis*-induced peri-implantitis model *in vitro*.

MATERIALS AND METHODS

1. Materials

Brain heart infusion (BHI) broth, yeast extract, bacto-agar, resazurin, cysteine HCl, hemin and vitamin K_1, 3-(4,5-dimethyl-2-thiazolyl)-2, 5-diphenyl-2H-tetrazolium bromide (MTT) and 2′,7′-dichlorofluorescin diacetate (DCFH-DA) were purchased from Sigma-Aldrich Chem. Co., (St. Louis, MO, USA). Benzenepentacarboxylic acid (BPBA), N,N,N′,N′-tetraacetylethylenediamine and terephthalic acid were purchased from TCI Chem. (Tokyo, Japan). Singlet oxygen sensor green (SOSG) was purchased from Invitrogen (Thermo Fisher Scientific Co. Ltd., Eugene, Oregon, USA). The live/dead cell staining kit was purchased from Biovision (Milpitas, CA, USA). Organic solvents such as ethyl alcohol and hexamethyldisilazane were as HPLC grade.

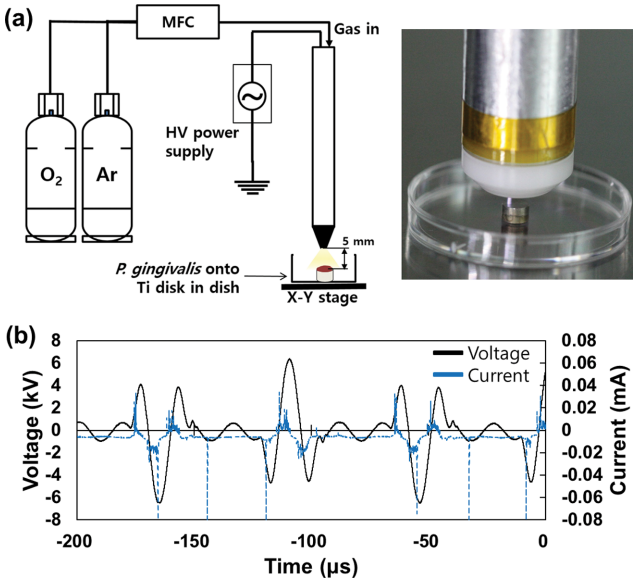

Fig. 1. (a) Schematic diagram of CAP experimental ap- paratus. Flow rate of Ar gas was 2 L/min. Discharge power adjusted at 5 W, 10 kV and 9.0 kHz. The distance was 5 mm from nozzle to Ti disks. (b) Oscilloscopic spectrum of plasma discharge.

2. CAP Equipment for Treatment of Bacteria

For treatment of bacteria onto Ti disks, we designed CAP apparatus as shown in Fig. 1. These are composed of a gas supply system, a plasma jet, a mass flow controller (MFC) and a high-voltage AC power supply. The discharge power was adjusted to 5 W and 10 kV. 2 L/min of Ar gas was supplied for plasma treatments from the gas supply system, and gas having higher than 99.9% purity was used for this experiment. Ti disks having bacteria were placed on the XY stage as shown in Fig. 1. The distance between the plasma jet nozzle and the top of the Ti disks was adjusted to 5 mm. The Ti disks were 5 mm diameter and 3 mm height.

3. Bacteria Culture

P. gingivalis (KCOM 2796) was supplied from Korean Collection for Oral Microbiology (Gwangju, Korea). BHI growth medium for *P. gingivalis* KCOM 2796 was as follows: 1 L solutions including 30 g of BHI broth, 5 g of yeast extract, 4.0 ml of resazurin solution (0.025% (w/v) in phosphate-buffered saline (PBS, pH 7.4, 0.01 M)), 0.5 g of cysteine HCl, 1.0 ml hemin solution (5 mg/ml in water) and 0.2 ml of vitamin K1 (10 mg/ml in water). This solution was adjusted to pH 7.2. For agar medium, bacto-agar (20 g) was added to growth medium. Bacteria were cultured under anaerobic condition (GasPak-EZ anaerobic container system; Becton Dickinson

Microbiology Systems, Cockeysville, MD, USA) for 1 day. The count of bacteria was evaluated by spectrophotometry in BHI medium containing 1×10^6 colony-forming units (CFU)/mL. The sterilized Ti discs were placed into 12 well plates and then bacteria were inoculated. These were incubated in an anaerobic environment for 3-5 days until bacterial confluence onto disk surface. Media were exchanged at intervals of 48 h during incubation.

4. Biofilm formation of *P. gingivalis* on the Ti disks

For antibacterial study of CAP apparatus, sandblasting with large grits and acid etched (SLA)-treated Ti disks were used as a model of dental implant. SLA-treated Ti disks were 5 mm diameter and 3 mm height in dimension. Onto these Ti disks, *P. gingivalis* was grown in an anaerobic condition for three days. *P. gingivalis* on the Ti disks was stained with live dye to verify as described below whether these bacteria are viable or not. For live/dead staining of bacteria, staining solution was prepared as follows: 1 μl live dye (1 mM) and 1 μl dead dye solution (1 mg/mL propidium iodide) (PI) was added to 1 ml staining buffer and then observed with a confocal laser scanning microscope under dark conditions (Zeiss LSM 800 confocal laser scanning microscope, Carl Zeiss Microscopy, NY, USA).

5. CAP Treatment and Colony-forming Unit Assay

P. gingivalis on the SLA-treated Ti disks as described before was carefully washed with sterile PBS (0.01 M, pH 7.4, Welgene) to remove the planktonic or loosely attached bacteria. The condition for CAP treatment was as follows: Ar gas flow rate of 2 L/min, voltage of 10 kV, and frequency of 9 kHz for 30, 60, 90, 120 and 180 s. After the treatment, treated samples were put into Eppendorf tubes containing 1.0 mL of PBS and then the remaining *P. gingivalis* on the SLA-treated Ti disks was detached with ultrasound for 5 min. Among obtained suspensions, 20 μl of this solution was smeared onto agar plates having BHI medium in the 10 cm dish, cultured in anaerobic condition, and the CFU number in the 10 cm dish was counted after incubation at 37 °C for 48 h.

6. OES Measurement in Plasma Jet Flame

To analyze optical emission spectra of the CAP, a fiber optic spectral analyzer (Avantes AvaSpec-ULS2048CL-EVO-RS, spectra range from 200 to 1,100 nm) was used to measure optical properties of plasma jet. An optical fiber (Avantes, Fiber-optic cable, FC-UV400-2) was placed from the nozzle of the plasma jet with a distance of 10 mm.

7. Electric Characterization of Plasma Discharge in CAP

Electric characterization of the system involved using a Tektronix MDO32 oscilloscope. The voltage and discharge current were measured by the high voltage probe (Tektronix P6015A, Beaverton, Oregon, USA) and current probe (Tektronix TCP0030A, Beaverton, Oregon, USA), respectively. Plasma power was calculated using software Tektronix 3-PWR oscilloscope software power measurement and analysis.

8. Observation of Ti Disks

For morphological observation of bacteria on the SLA-treated Ti disks, bacteria on the SLA-treated Ti disks were treated as follows: samples were immersed into mixed solution of paraformaldehyde (2.5%, v/v) and glutaraldehyde (2.5%, v/v) for 3 h. They were washed with PBS (pH 7.4, 0.01 M) and then immersed again into OsO_4 (1%, w/v in distilled water) for 30 min. Following this, they were washed with PBS and then dehydrated with ethyl alcohol/water mixtures. For the dehydration process, samples were immersed into these solutions for 5 min each ethyl alcohol/water mixtures with 70% (v/v), 90% (v/v), 95% (v/v) and 100% (v/v), respectively. Dehydrated samples were immersed into hexamethyldisilazane solution for 10 min and then dried at room temperature. Samples were observed with field-emission scanning electron microscope at 25 kV (FE-SEM, S-4800, Hitachi Instruments Ltd., Tokyo, Japan).

9. Live and Dead Cell Staining for Bacteria

Live-dead cell staining kit (Biovision Inc., Milpitas, CA, USA was used for live/dead staining of bacteria. Live Dye™, a cell-permeable green fluorescent dye, was used to stain live bacteria at 488 nm of excitation wavelength and 518 nm emission wavelength. Propidium iodide (PI), a non-permeable red fluorescent dye, was used to stain dead cells at 488 nm of excitation wavelength and 615 nm emission wavelength. Staining solution was prepared as follows: 1 μl live dye (1 mM) and 1 μl dead dye solution (1 mg/mL propidium iodide) (PI) was added to 1 ml staining buffer. To observe the viability of bacteria, bacteria on the surface of SLA-treated Ti disks were treated with CAP equipment as described above. Then, bacteria on the SLA-treated Ti disks were briefly washed with PBS and incubated for 10 min with 1 mL of the live/dead cell staining solution at 37 °C. Following this, bacteria on the Ti disks were observed with a confocal laser scanning microscope under dark conditions (Zeiss LSM 800 confocal laser scanning microscope, Carl Zeiss Microscopy, NY, USA).

10. Cell Culture

HGF-1 cells were purchased from American Type Culture Collection (ATCC, Manassas, USA). HGF-1 cells were maintained in DMEM medium supplemented with 10% heat-inactivated FBS and 1% penicillin/streptomycin at 37 °C in a 5% CO_2 incubator.

To study the CAP effect on the viability of cells, 5×10^5 cells were seeded in 35 mm dish with media and then cultured overnight in the 5% CO_2 incubator. After that, cells were washed with phosphate buffered saline (PBS, pH 7.4, 0.01 M) and replaced with 2 ml of serum-free media. Then, cells were treated with CAP equipment (Fig. 1(a)) at similar condition as described in colony-forming assay with CAP apparatus (flow rate: 2 L/min, Argon gas; oxygen gas ratio, 5%) at a 3 cm distance from the media. 24 h later, viability of cells was evaluated with MTT cell proliferation assay. 100 μl of MTT solution (5 mg/ml, PBS) was added to dishes and then incubated for 3 h in the 5% CO_2 incubator at 37 °C. Following this, supernatants were removed and then 500 μl DMSO was added to dissolve formazan crystal in viable cells. This was measured at 560 nm with a microplate reader (EPOCH, BioTek Instruments Inc., Winooski, VT., USA). Four different plates of cell culture were used to calculate average ±S.D. (standard deviation).

11. ROS/RNS Assay

Singlet oxygen produced from CAP equipment in the aqueous solution was monitored with the SOSG reagent. SOSG stock solution was prepared by dissolving it in methyl alcohol (5 mM). 1 ml PBS (0.01 M, pH 7.4) was exposed to plasma jet with CAP equipment with various conditions. To this solution, 1 μl SOSG stock solution was added and then fluorescence intensity was measured at 400 nm of excitation wavelength and 525 nm of emission wavelength using fluorescence spectrophotometer (RF-5301PC, Shi-

madzu Co., Kyoto, Japan). This procedure was carried out under dark conditions. ROS values are average ±S.D. (standard deviation) from individual four measurements.

Hydroxyl radicals (OH^-) were measured by BPBA method as reported by Si et al. [20]. Briefly, 1 ml PBS (0.01 M, pH 7.4) was exposed to plasma jet with CAP equipment with various conditions. To this solution, 1 ml of BPBA solution (0.8 mM in deionized water) was added (final concentration of BPBA=0.4 mM) and then fluorescence intensity was measured using fluorescence spectrophotometer (RF-5301PC, Shimadzu Co., Kyoto, Japan) (λ_{ex}=311 nm, λ_{em}=435 nm). All procedures were performed at 80 °C.

Nitric oxide produced from CAP equipment was measured as follows: 1 ml PBS (0.01 M, pH 7.4) was exposed to plasma jet with CAP equipment with various conditions. To this solution, 1 ml of Griess reagent [1% (w/v) sulfanilamide, 0.1% (w/v) naphthylethylenediamine in 2.5% (v/v) phosphoric acid] and then reacted for 10 min at dark condition. This was measured with microplate reader (BioTek, Winooski, VT, USA) at 540 nm.

Intracellular ROS accumulation in HGF cells was measured with DCFH-DA method. 5×10^5 cells were seeded in 35 mm dish with media and then cultured overnight in the 5% CO_2 incubator. The cells were washed with phosphate buffered saline (PBS, pH 7.4, 0.01 M) and replaced with 2 ml of serum-free media. Then, cells were treated with CAP equipment (Fig. 1(a)) at similar condition as described in colony-forming assay with CAP apparatus (flow rate: 2 L/min, Argon gas; oxygen gas ratio, 5%) at a 3 cm distance from the media. Following this, DCFH-DA (PBS, final concentration: 20 μM) was added to cell culture and further incubated for 2 h at 37 °C. Cells were washed with PBS, treated with trypsin-EDTA and then harvested by centrifugation. Cells in 500 μl fresh phenol red free media were then used to measure intracellular ROS level using Infinite M200 pro microplate reader (Tecan Trading AG, Männedorf, Switzerland) to measure intracellular ROS level (Excitation wavelength, 485 nm; emission wavelength, 535 nm).

12. Statistical Analysis

To analyze statistical significance, a one-way analysis of variance (ANOVA) followed by the Tukey test was employed using GraphPad Prism 9 (GraphPad Software LLC., San Diego, CA, USA). The minimum of significance was evaluated as $p<0.05$.

RESULTS

1. CAP Equipment and Optical Emission Spectroscopy (OES) Analysis

For treatment of *P. gingivalis* biofilm, CAP equipment was designed as shown in Fig. 1. The distance between nozzle and Ti surface having *P. gingivalis* was adjusted to 5 mm and the flow rate of Ar gas was adjusted to 2 L/min. Prior to treating *P. gingivalis* biofilm, frequency and power were measured as abbreviated in Table 1. As shown in Table 1, true power of plasma jet was gradually increased according to the increase of energy levels and, practically, 90-90 of intensity-energy ratio is the limit of plasma power of CAP apparatus used in this study. These results might be due to that increase of voltage was blunted at 90-90 vs. 90-70 compared to 90-70 vs. 90-50, and then the power for changes of oxygen to ROS was also blunted. Fig. 2 shows typical OES spectrum of plasma jet plume from CAP equipment. In measurement of OES, the peaks of OH and O band were sparsely measured with OES equipment. Then, the differences in the peak intensity of OH and O band simply showed the typical spectrum of CAP. As shown in Fig. 2 are the peaks of Ar^+, OH and O^- ions observed in the UV range (200 nm-400 nm) and visible range (690 nm-950 nm). The peaks of OH and O^- ions increased according to the increase of energy level as shown in Fig. 2. Furthermore, the OH and O^- ions also increased when relative volume of oxygen supply was decreased (Fig. S1).

Table 1. Characterization of frequency and power of CAP

Intensity-energy level ratio	Peak-Peak (kV)	Frequency (kHz)*	True power (W)
90-50	11.04	9	3.498
90-70	13.30	9	6.387
90-90	13.91	9	6.994

* Frequency was measured as 111 μs. 1/111 μs=9.009 kHz.

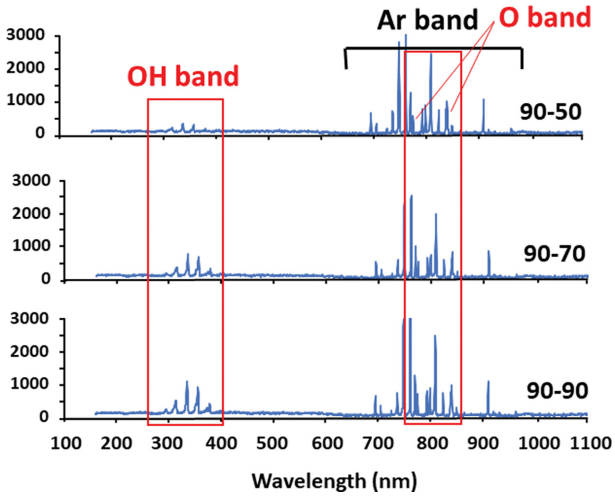

Fig. 2. Typical optical emission spectroscopy (OES) spectrum of CAP plume according to the energy level.

2. ROS Formation of CAP Equipment

Since ROS/RNS such as singlet oxygen ($^1O_2$), hydroxyl radical (OH^-) and nitrogen oxide (NO) induces oxidative stress and then suppresses bacterial growth, the capacity of CAP apparatus in the ROS/RNS production was evaluated as the generation of singlet oxygen, hydroxyl radical and nitrogen oxide in the aqueous system. Fig. 3 shows the generation of singlet oxygen ($^1O_2$), hydroxyl radicals (OH^-) and nitric oxide (NO) in PBS using CAP treatment to test ROS/RNS-producing capacity. As shown in Fig. 3(A(a)), (B(a)) and (C(a)), the $^1O_2$, OH^- and NO generation according to the treatment time in an aqueous solution, indicated that ROS/RNS level was gradually increased according to the treatment time. Furthermore, ROS/RNS level also gradually increased according to the energy level as shown in Fig. 3(A(b)), (B(b)) and (C(b)). These results indicate that CAP apparatus efficiently produced ROS in the aqueous solution. Especially, the difference of contents of ROS/RNS generation was relatively higher at 90-70 vs. 90-90 than other treatment regimen. These results might be due to that

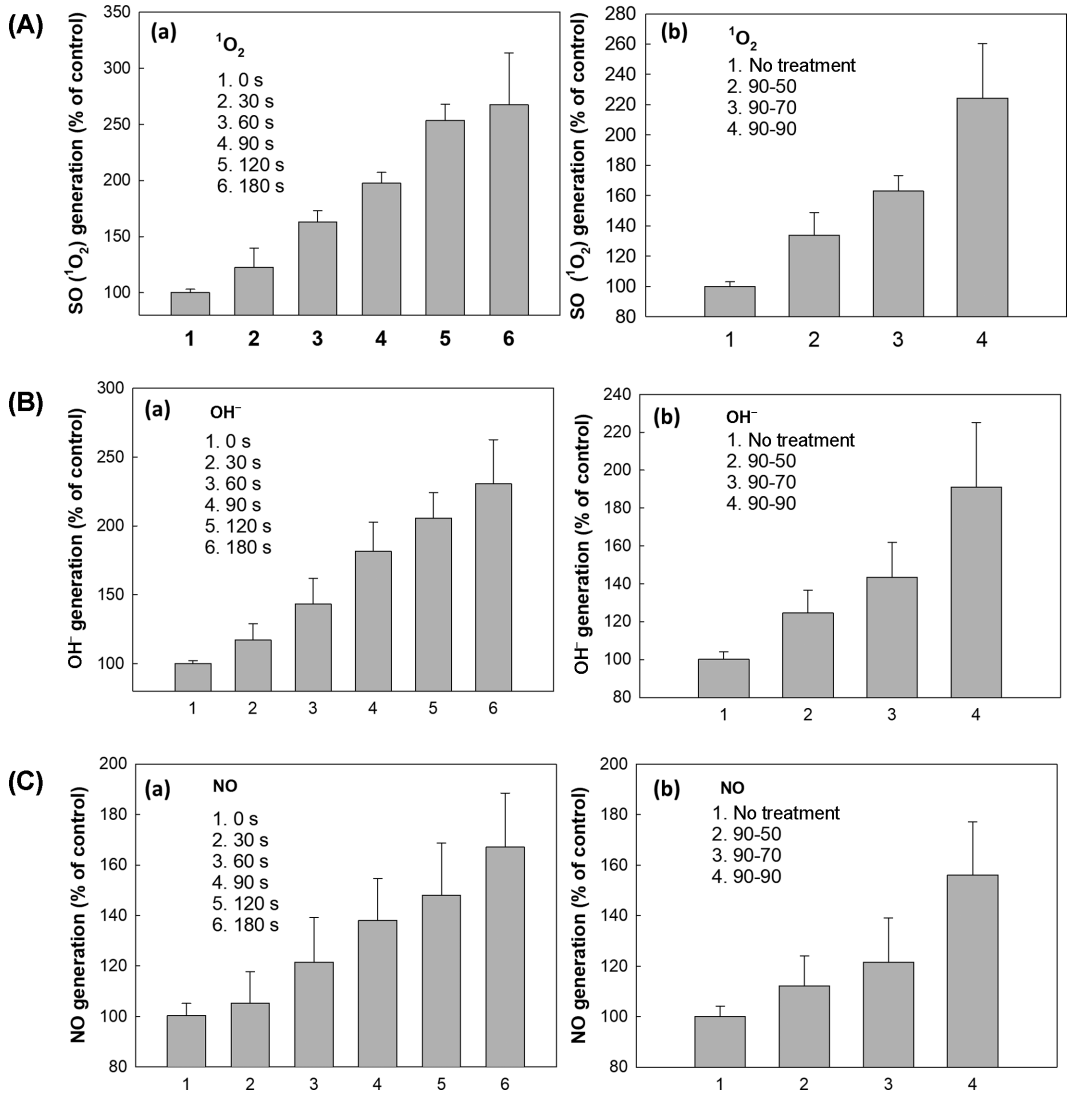

Fig. 3. Generation of various ROS. (A) singlet oxygen ($^1O_2$), (B) hydroxyl radical (OH^-) and (C) nitric oxide (NO) from CAP equipment in PBS (0.01 M, pH 7.4). (a) The effect of treatment time (Intensity, 90; energy level, 70). (b) The effect of plasma power (treatment time, 60 s). The ratio of oxygen supply was 5% in this experiment.

90-90 has maximum power to produce ROS/RNS than other conditions.

3. Antibacterial Capacity of CAP Equipment

Since antibacterial potential of CAP is basically related to the inhibition of *P. gingivalis*-induced biofilm formation on the dental implant, the antibacterial activity of CAP equipment was evaluated with *P. gingivalis*-covered Ti disks. Furthermore, *P. gingivalis*-covered Ti disks were prepared for imitation of biofilm-formed dental implant.

For antibacterial study of CAP apparatus, SLA-treated Ti disks were used as a model of dental implant as shown in Fig. 4. SLA-treated Ti disks are 5 mm in diameter and 3 mm in height (Fig. 4). Onto these Ti disks, *P. gingivalis* was grown in an anaerobic condition as shown in Fig. 5. As shown in Fig. 5(a), FE-SEM photographs show that *P. gingivalis* was placed on the surface of Ti disks, overlapping each other and then forming biofilm-like shapes. Fig. 5 shows that *P. gingivalis* on the Ti disks was stained with live dye to verify whether these bacteria are viable (Fig. 5(b)). As shown in Fig. 5(b), viable bacteria (green) were successfully grown onto the Ti disks. It seems that the number of dead bacteria is practically negligible because red fluorescence color was not observed as shown in Fig. 5(b). Otherwise, Ti disks without *P. gingivalis* showed none of the bacteria (Fig. 5(c)). These results indicate that *P. gingivalis* can be forming biofilms onto the Ti disks as similar to bacterial biofilm on the dental implant.

Fig. 6 shows the colony-forming unit (CFU) assay using *P. gingivalis* to study the potential of biofilm eradication of CAP apparatus. For this experiment, *P. gingivalis* biofilm formed onto the Ti disks was treated with CAP apparatus and then Ti disks were washed with PBS. The detached bacteria were grown in agar plate in an anaerobic condition. As shown in Fig. 6(a), the number of CFU of *P. gingivalis* after treatment gradually decreased according to the treatment time and the energy level. Fig. 6(b) and (c) shows the estimated CFU number of four independent experiments from

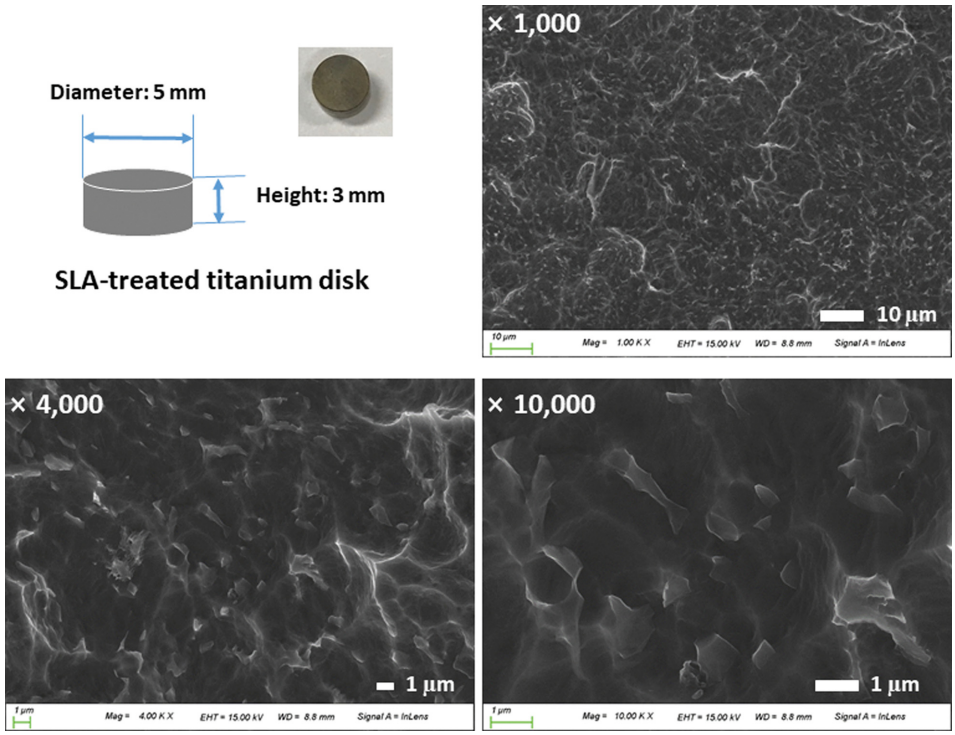

Fig. 4. FE-SEM images of surface morphology of SLA-treated Ti disks. Samples were observed with FE-SEM at 25 kV. Magnification was each observation condition with FE-SEM. White bar of ×1,000, ×4,000 and ×10,000 indicates size of 10 μm, 1 μm and 1 μm, respectively.

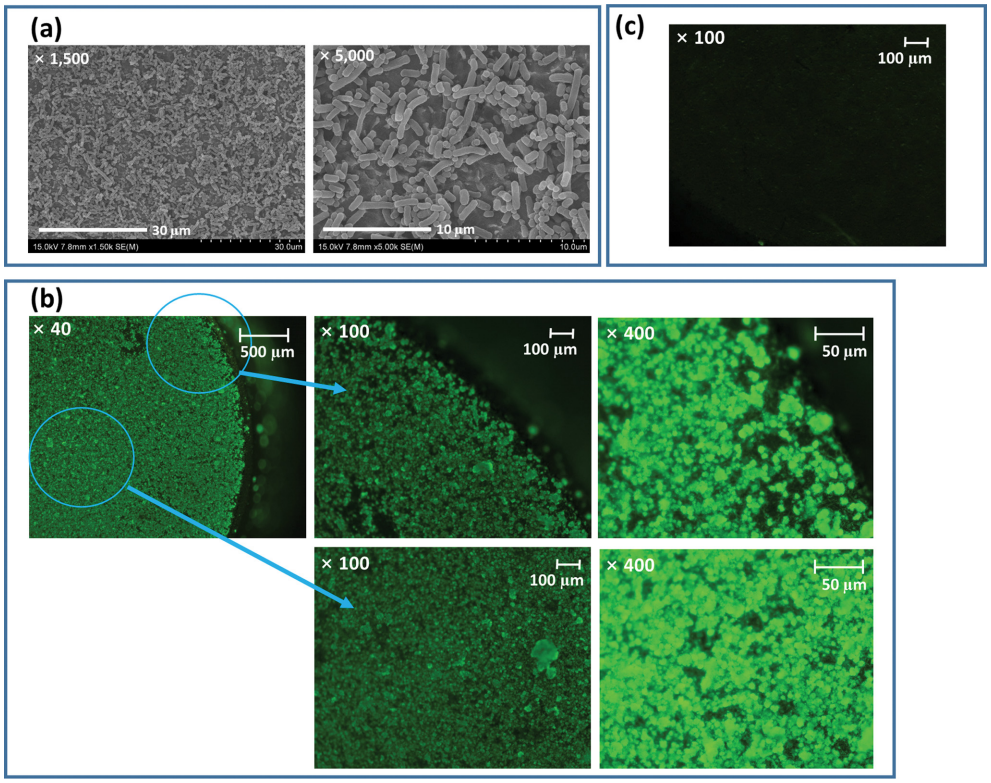

Fig. 5. Morphological observation of biofilm formation on the surface of Ti disks. (a) FE-SEM photographs. (b) Fluorescence observation of *P. gingivalis* on the surface of Ti disks. (c) No fluorescence images observed from empty Ti disk surface. Live Dye™ was used to live bacteria (488 nm of excitation wavelength and 518 nm emission wavelength) and propidium iodide (PI) was used to stain dead bacteria (488 nm of excitation wavelength and 615 nm emission wavelength).

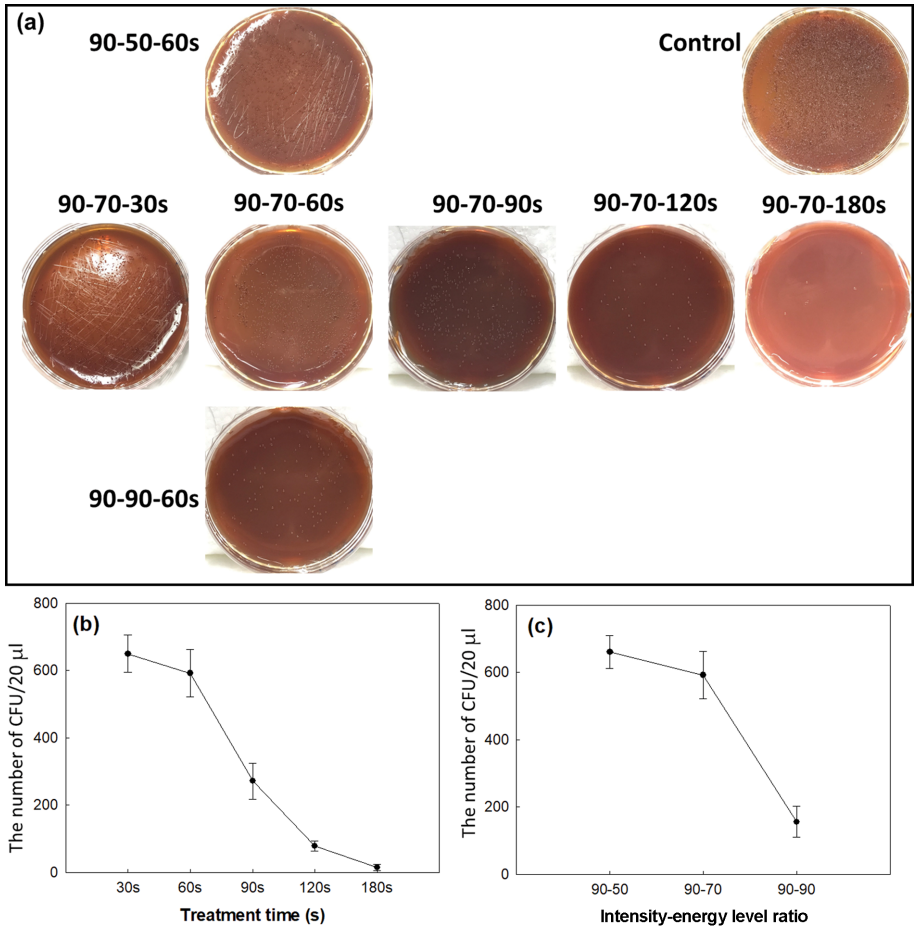

Fig. 6. Colony-forming unit (CFU) assay of *P. gingivalis*. (a) Photographs of surviving bacteria after CAP treatment. (b) The effect of treatment time on the survivability of *P. gingivalis* (90-70 in Table 1). (c) The effect of plasma power on the survivability of *P. gingivalis* (Treatment time: 60 s). The treated samples were detached into 1.0 mL of PBS by sonication. Then, 20 μl of this solution was smeared onto agar plates having BHI medium in the 10 cm dish, cultured in anaerobic condition, and the CFU number in the 10 cm dish was counted.

treatment time and energy level, respectively.

To observe live and dead bacteria, viable and/or dead *P. gingivalis* on the Ti disks was stained with green dye for live bacteria and red dye for dead bacteria as shown in Fig. 7 and Fig. S2. As shown in Fig. 7, live bacteria were observed as a green dye, while dead bacteria were observed as red dye. When tretament time was increased, dead bacteria as a red color were relatively increased according to the treatment time, while control or short treatment time revealed higher degree of viable bacteria as shown in Fig. 7. These results indicate that the CAP apparatus has the potential to eradicate *P. gingivalis* biofilm in the Ti disks. Furthermore, these results also indicate that CAP apparatus can be used to eradicate bacterial biofilm on implant surfaces.

Fig. 8 shows the effect of CAP apparatus on the viability of HGF-1 human gingival fibroblast cells. These experiments were to study the potential adverse influences of plasma jet on normal cells or tissues in the gingival region even though most of the cells are surrounded by extracellular matrix. As shown Fig. 8(a), the viability of HGF-1 cells gradually decreased according to the treatment time and the energy level. Especially, the viability of HGF-1 cells was significantly inhibited at longer than 120 s. Furthermore, the higher energy level induced gradual inhibition of HGF-1 cell viability. These inhibitory effects of CAP apparatus against HGF-1 cells were due to the ROS generation in an aqueous solution by CAP treatment as shown in Fig. 8(b); intracellular ROS level was gradually increased according to the treatment time and the energy level. Even though plasma irradiation condition at 90-90 resulted in higher ROS level and increased bactericidal effect, the viability of HGF-1 cells was also lower than that of other protocols. Furthermore, these results indicated that CAP apparatus produces ROS in an aqueous solution and then the generated ROS can potentially affect the viability of normal cells in the gingiva. In this study, the appropriate condition of CAP irradiation for eradication of biofilm can be evaluated as 90-70 of intensity/energy level ratio for 60 s, and then the dental implant can be repetitively irradiated with CAP for complete eradication of biofilm. Furthermore, CAP treatment also increases the temperature of an aqueous solution and may affect the viability of normal cells, as shown in Fig. S3(a) and (b). Also, these results indicate that appropriate time of CAP treatment for eradication of *P. gingivalis* biofilm on the Ti implant surface is import-

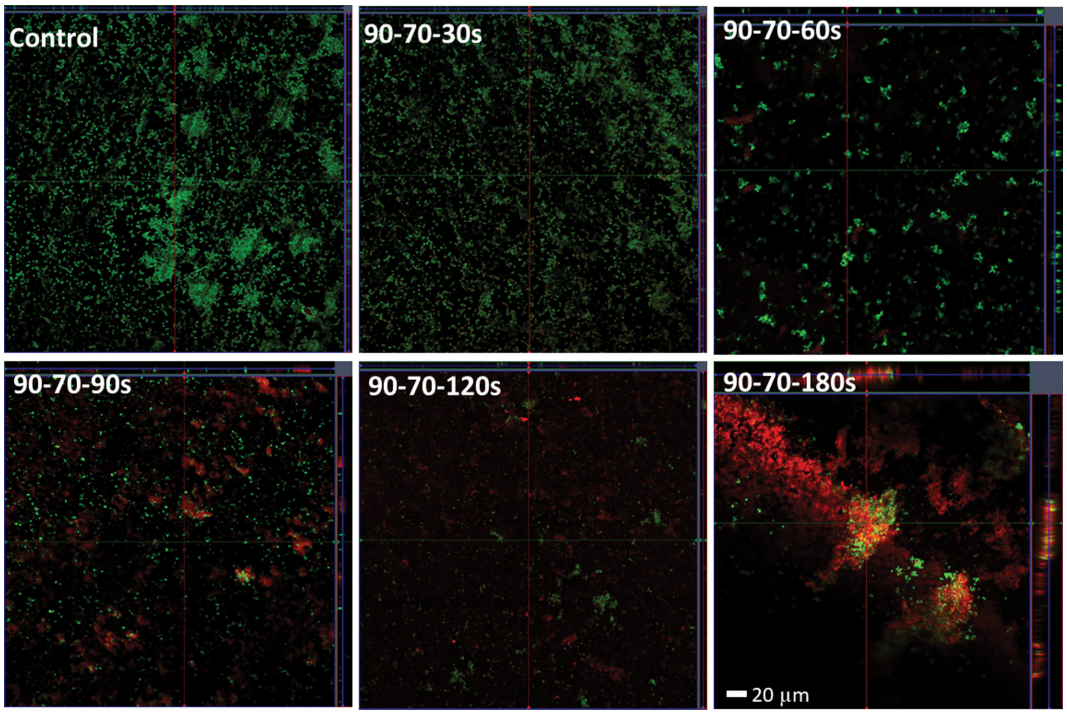

Fig. 7. The effect of treatment time of CAP apparatus on the viability of *P. gingivalis* on the Ti disks. *P. gingivalis* on the Ti disks was treated with CAP apparatus and then stained with live and dead cell dye of *P. gingivalis*. Green and red color represents live and dead bacteria, respectively.

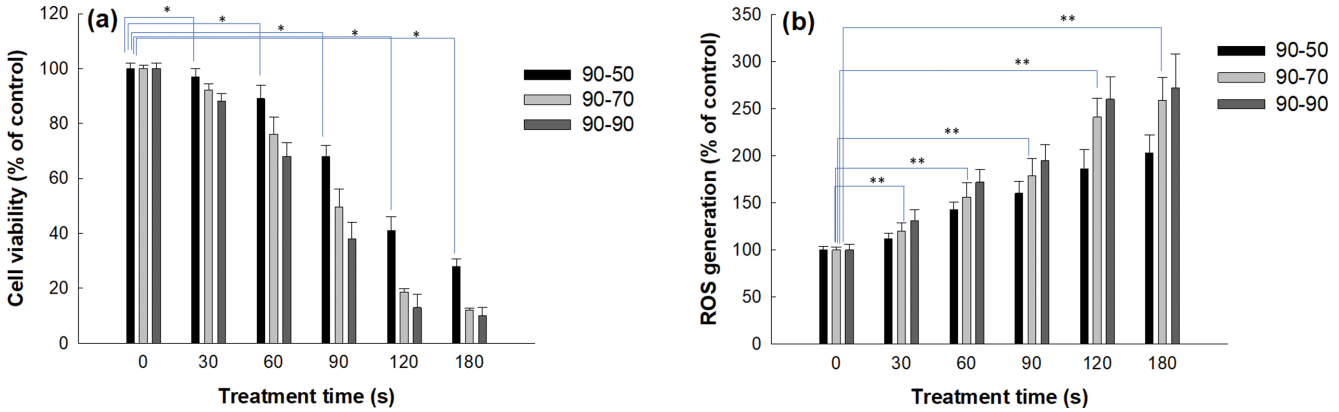

Fig. 8. Viability and intracellular ROS level of HGF-1 cells after treatment of CAP. The effect of treatment time and energy level on the viability of HGF-1 cells (a) the intracellular ROS level in HGF-1 cells (b). Cell viability was evaluated by MTT-cell proliferation assay. Intracellular ROS level was measured with DCFH-DA method. *, ** indicates comparison between no-treatment (0 time) vs. each tretament times. A one-way ANOVA followed by the Tukey test was employed to analyze the statistical significance. The statistical analysis was $p<0.05$ as a the minimum of significance.

ant even though the longer the treatment time of CAP was more effective to eradicate *P. gingivalis* biofilm from the Ti disks.

DISCUSSION

The plasma jet has been extensively investigated in the biomedical field [21-24]. Practically, the plasma jet by generated by CAP or NTP has a Janus (two-faced) characteristic, i.e., the CAP apparatus produces ROS in the biological system and then the level of produced ROS in the biological system determines the fate of cells or bacteria. For example, the CAP apparatus enhances periodontal wound healing rate through control of cell viability and down-regulation of apoptosis [21]. At low dose of CAP irradiation, redox stress enhances the proliferation rate of normal cells through the stimulation of key genes in fibroblasts, and these events induce initiation of the skin repair process [22]. Furthermore, excessive amount of ROS produced by CAP irradiation also kills cancer cells at an appropriate dose [23]. Mahdikia et al. reported that hydrogen peroxide, nitrite and nitrate produced in water by CAP irradiation induce apoptosis and death of B16F10 melanoma carcinoma cells

[23]. We also previously reported that CAP treatment significantly increases intracellular ROS level and then induces apoptosis of oral squamous carcinoma cells [24]. The principal mechanism of CAP treatment against biological systems is practically ROS-generation capacity. ROS-generated from CAP apparatus has a Janus-faced function against biological systems, i.e., ROS protects or damages biological system depending on the series of reactive species, the quantity of formed species, and their location in subcellular region [25]. Thus, this Janus-faced role of ROS can be used to kill pathogens or cancer cells and to activate key molecules for wound healing. Especially, CAP jet produces various reactive species.

Gargling and mouth wash using antibiotics, such as povidone iodine and cetylpyridinium chloride, is difficult to eradicate biofilm on the implant and/or teeth [26,27]. The use of antibiotics for mouthwash has a drug-resistant problem [26]. Especially, antibiotic is difficult to deliver to the biofilm on the teeth or implant through mouthwash. For these reasons, mechanical removal is still believed to be a suitable candidate for periodontal disease, such as peri-implantitis and/or periodontitis [28]. However, mechanical disruption of biofilm may cause immunological shifts in patients [29]. Furthermore, mechanical disruption of biofilm is associated with the remaining problem of biofilm dysbiosis and host inflammation in some patients [29]. Otherwise, ultrasonic devices for periodontal disease also have a risk of recurrence problem [30]. Furthermore, CAP is known to have potential of biofilm eradication formed on the surface of dental film, and then kills pathogens on the dental implant or teeth [17-19]. Pathogens such as *P. gingvalis* form biofilm on the surface of dental implant, and biofilms on dental implants are typically composed of a complex extracellular matrix of polymeric substances. ROS/RNS can be used to attenuate biofilm on the surface of dental implant or teeth [19,31]. CAP apparatus generates ROS/RNS, attenuates physicochemical/mechanical properties of biofilm and then suppresses growth of pathogenic bacteria [19,31-33]. That is, ROS/RNS produced by treatment with CAP has bactericidal effect and can be used to eradicate biofilm formed by peri-implantitis. Since CAP treatment is limited to 100 μm from the biological surface, CAP treatment is primarily limited to disease of epidermal disorders or bacterial biofilm [34]. Furthermore, the lifetime of ROS generated by treatment with CAP is normally very short in the biological system [35]. Especially, short-lived reactive species such as $O^{\bullet}$, $O_2^{\bullet-}$, and $^{\bullet}OH$ ions have higher efficacy in inactivation of bacteria than those of long-lived reactive species, even though CAP jet produces both long-lived and short-lived species [35]. Xu et al., also reported that short-lived ROS, such as singlet oxygen, hydroxy radical and superoxide anion, is produced by CAP jet in water and, furthermore, singlet oxygen has highest efficacy in inactivation of bacteria [36]. Therefore, appropriate conditions for eradication of biofilm on the dental implant have to be decided for application of CAP in human uses. The investigations for the ROS generation by CAP equipment and its efficacy in biofilm eradication efficiency in peri-implantitis are still few [16,37]. Abnormal level of ROS/RNS can be used for eradication of bacteria and/or cancer cells [36,37]. For example, Thakur et al. reviewed that ROS produced by nanoceria has excellent antibacterial activity [38]. Also, Jang et al. reported that ROS-producing chemical agents such as piperlongumine generate oxidative stress in epithelial cancer [39]. In their report, piperlongumine produced ROS excessively in cancer cells and then abnormal ROS level induced apoptosis of cancer cells. Su et al. reported that ROS formation in the aqueous system contributes to disrupting bacterial membrane integrity and then inhibits the viability of bacteria [40]. Especially, Bekeschus reviewed that plasma technology has been used to treat wound healing through inactivation of pathogen [41]. Furthermore, CAP treatment is known to increase intracellular ROS/RNS level and then effectively eliminates antibiotic-resistant Staphylococcus aureus in RAW 264.7 cells [42]. Since CAP equipment is acceptable for treatment of surface or near-surface of biological systems and biomaterials, CAP equipment for eradication of *P. gingivalis* biofilm on the surface of Ti disks was studied. Our group previously reported that atmospheric-pressure plasma jet (APPJ) can be used to sterilize *Staphylococcus aureus* efficiently [43]. Furthermore, APPJ induces the rupture of bacterial cell morphology and then inhibits their growth. Kim et al. reported that cold atmospheric microwave plasma is effective to eradicate planktonic bacteria and biofilm formation of *P. aeruginosa* [44]. Our results showed that *P. gingivalis* biofilm can be eradicated by treatment with CAP apparatus as shown in Fig. 6 and 7. These results were associated with ROS generation by CAP apparatus as shown in Fig. 3. Furthermore, the increase of hydrophilicity of Ti disks according to the increase of CAP treatment time (Fig. S4) might be also affecting the decrease of the number of CFU and live bacteria, as shown in Fig. 6 and 7. Yang et al., also reported that plasma jet treatment using helium efficiently inhibits the growth of bacteria and forming of biofilm by *Streptococcus mutans*/*P. gingivalis* [16]. In their report, the viability of bacteria showed treatment time-dependent decrease and then dead bacteria gradually increased in live/dead cell staining assay. Our results also showed that dead bacteria were gradually increased according to the increase of treatment time as shown in Fig. 7. Lee et al. also reported that helium-based plasma jet efficiently inhibits the viability of bacteria on Ti disks and then increases staining of dead bacteria according to the increase of treatment time [45]. In our results, the increase of ROS level in the aqueous environment contributed to the death of bacteria as shown in Fig. 3 and Fig. 6. The increase of treatment time induced increase of singlet oxygen as one of ROS level in the aqueous solution and then affected the viability of bacteria on the Ti disks. ROS-enriched aqueous solutions generated by plasma jet have effectiveness to inhibit microbial infection [46,47]. As shown in Fig. 3(A(b)), (B(b)) and (C(b)), the difference in contents of ROS/RNS in aqueous solution between 90-70 and 90-90 was relatively higher than those of 90-50 and 90-70, while the difference of OH/O band peaks in Fig. 2 was relatively small. These results might be due to that ROS/RNS ions such as $^1O_2$, OH^- and NO ion rapidly disappear in the aqueous media with the unit of a second. These might be affecting the measurement and the results of ROS/RNS generation. Small number of bacteria survived at 120 s or 180 s (Fig. 6(b)) in spite of that 120 s or 180 s is a quite long period of treatment time. These results might be due to that bacteria were grown on the Ti surface layer by layer and then formed a colony and piled up onto the surface, as shown in Fig. 5(a). Then, during CAP treatment, dead bacteria on upper layer might become a shield for bacteria in the lower layer, and then small number of bacteria might survive at

120 s or 180 s treatment period.

Cubas et al. reported that inactivation of *Escherichia coli* (*E. coli*) occurred at air/Ar mixture (1/1, v/v) through production of reactive species in the aqueous solution by NTP discharge [48]. They argue that Ar gas induces only partial inactivation of *E. coli* and then air/Ar mixture is required to inactivate *E. coli*. In our results, normal cells such as HGF-1 cells can be affected by ROS generation from CAP apparatus, which is required to inhibit the viability of bacteria sufficiently, as shown in Figs. 3, 6, 7 and 8. That is, ROS formation was gradually increased by treatment time and energy levels of CAP apparatus, and this status induced lower viability of HGF-1 cells *in vitro*, as shown in Fig. 8. Furthermore, as one of reactive species, ozone can be formed during irradiation with CAP apparatus [49]. The increase of oxygen gas ratio in the Ar plus oxygen gas induces ozone formation and then ozone as one of reactive species by CAP irradiation induces apoptosis/necrosis of 3T3 fibroblast cells [50]. In future study, we will also investigate precisely about the effect of ozone formation during CAP treatment in the biological system. In fact, normal cells are not significantly affected by irradiation of plasma jet because cells are surrounded by extracellular matrix (ECM) at the condition of *in vivo* state. Then, CAP treatment may have only indirect cytotoxicity against normal cells. Partecke et al. reported that the penetration depth of plasma jet was less than 48.8±12.3 μm in the Colo-357 tumor cells-based chorio-allantoic membrane model and then it induces apoptosis of tumor cells [51]. Furthermore, Nastasa et al. reported that long-term exposure to plasma-activated water does not cause adverse effects, i.e., organs and tissues of mice were not changed in histopathological examination with 90 days uptake of plasma-activated water [52]. In our study, HGF-1 cells were irradiated with CAP in the presence of media because normal cells are generally surrounded by extracellular matrix and are not directly exposed to plasma irradiation. Furthermore, appropriate treatment time and energy levels can be determined to maximize eradication efficiency of bacterial biofilm and minimize harmful effect against normal cells through *in vivo* experiment.

CONCLUSION

CAP apparatus was designed to eradicate biofilm formation by *P. gingivalis* for application in peri-implantitis treatment. The true power of plasma discharge from CAP apparatus was gradually increased according to the increase of intensity/energy level ratio. OES of plasma jet plume from CAP equipment showed that the peaks of Ar^+, OH and O^- ions were observed in the UV range (200 nm-400 nm) and visible range (690 nm-950 nm). Biofilm of *P. gingivalis* was formed onto the Ti disks and viability of *P. gingivalis* was confirmed. Production of ROS in the aqueous solution by CAP apparatus was gradually increased according to the treatment time and energy level. The increased ROS level induced a decrease of surviving *P. gingivalis* according to treatment time and energy level. Furthermore, CAP treatment of *P. gingivalis* biofilm on the Ti disks also induced death of bacterial cells. Longer treatment time and higher energy level of CAP apparatus resulted in decrease of HGF-1 cell viability. Then, appropriate treatment time and energy level is required to maximize bactericidal effect with minimized cytotoxicity against normal cells or tissues. Practically, 6.387 W of plasma power was considered as an appropriate treatment condition and treatment time should be less than 60 s to diminish normal cell cytotoxicity. We suggest that CAP apparatus is a promising candidate to eradicate biofilm with antibacterial efficacy through ROS/RNS generation from CAP apparatus.

ACKNOWLEDGEMENT

This work was supported by the National Research Foundation of Korea (NRF) grant funded by the Korea government (MSIT) (No. 2020R1A2C2008540).

NOTES

The authors declare no competing financial interest.

NOMENCLATURE

Symbols

°C : degree centigrade
h : hour
min : minute
s : second
ms : millisecond
μs : microsecond
l : liter
ml : milliliter
μl : microliter
mg : milligram
μg : microgram
mol : mol
mA : milliampere
kV : kilovoltage
kHz : kilohertz

Abbreviations

CAP : cold atmospheric plasma
ROS : reactive oxygen species
RNS : reactive nitrogen species
Ti : titanium
OES : optical emission spectroscopy
HGF-1 : human gingival fibroblast-1
UV-VIS : ultraviolet-visible
Ar : argon
OH : hydroxide
O^- : oxygen ion
NO : nitrogen oxide
SO : singlet oxygen
nm : nanometer
CFU : colony-forming unit
MTT : 3-(4,5-dimethyl-2-thiazolyl)-2, 5-diphenyl-2H-tetrazolium bromide
DCFH-DA : 2′,7′-dichlorofluorescin diacetate
BPBA : Benzenepentacarboxylic acid
SOSG : Singlet oxygen sensor green

PBS : phosphate-buffered saline
BHI : Brain heart infusion
SLA : sandblasted with large grits and acid etched
FE-SEM : field-emission scanning electron microscope
PI : propidium iodide
DMEM : Dulbecco's modified eagle medium
FBS : Fetal bovine serum
CO_2 : carbon dioxide

SUPPORTING INFORMATION

Additional information as noted in the text. This information is available via the Internet at http://www.springer.com/chemistry/journal/11814.

REFERENCES

1. D. Clark, E. Kotronia and S. E. Ramsay, *Periodontol 2000*, **87**, 143 (2021).
2. G. N. Belibasakis, G. Charalampakis, N. Bostanci and B. Stadlinger, *Adv. Exp. Med. Biol.*, **830**, 69 (2015).
3. P. C. Passarelli, A. Netti, M. A. Lopez, E. F. Giaquinto, G. De Rosa, G. Aureli, A. Bodnarenko, P. Papi, A. Starzyńska, G. Pompa and A. D'Addona, *Antibiotics (Basel)*, **10**, 1298 (2021).
4. R. Matthes, L. Jablonowski, B. Holtfreter, C. Pink and T. Kocher, *Odontology*, **109**, 780 (2021).
5. N. Emanuel, E. E. Machtei, M. Reichart and L. Shapira, *Quintessence Int.*, **51**, 546 (2020).
6. P. Ramburrun, N. A. Pringle, A. Dube, R. Z. Adam, S. D'Souza and M. Aucamp, *Materials (Basel)*, **14**, 3167 (2021).
7. D. Braný, D. Dvorská, E. Halašová and H. Škovierová, *Int. J. Mol. Sci.*, **21**, 2932 (2020).
8. M. Izadjoo, S. Zack, H. Kim and J. Skiba, *J. Wound Care*, **27**(Sup9), S4 (2018).
9. G. Isbary, T. Shimizu, Y. F. Li, W. Stolz, H. M. Thomas, G. E. Morfill and J. L. Zimmermann, *Expert Rev. Med. Devices*, **10**, 367 (2013).
10. P. M. Girard, A. Arbabian, M. Fleury, G. Bauville, V. Puech, M. Dutreix and J. S. Sousa, *Sci. Rep.*, **6**, 29098 (2016).
11. F. Girard, M. Peret, N. Dumont, V. Badets, S. Blanc, K. Gazeli, C. Noël, T. Belmonte, L. Marlin, J. P. Cambus, G. Simon, N. Sojic, B. Held, S. Arbault and F. Clément, *Phys. Chem. Chem. Phys.*, **20**, 9198 (2018).
12. Y. Li, K. Sun, G. Ye, Y. Liang, H. Pan, G. Wang, Y. Zhao, J. Pan, J. Zhang and J. Fang, *J. Endod.*, **41**, 1325 (2015).
13. D. Küçük, L. Savran, U. K. Ercan, Z. B. Yarali, O. Karaman, A. Kantarci, M. Sağlam and S. Köseoğlu, *Clin. Oral Investig.*, **24**, 3133 (2020).
14. B. Kusakci-Seker, H. Ozdemir and S. Karadeniz-Saygili, *Clin. Oral Investig.*, **25**, 6949 (2021).
15. G. M. G. Lima, A. C. Borges, T. M. C. Nishime, G. F. Santana-Melo, K. G. Kostov, M. P. A. Mayer and C. Y. Koga-Ito, *Molecules*, **26**, 5590 (2021).
16. Y. Yang, M. Zheng, Y. Yang, J. Li, Y. F. Su, H. P. Li and J. G. Tan, *Clin. Oral Investig.*, **24**, 1465 (2020).
17. Y. Hong, J. Zeng, X. Wang, K. Drlica and X. Zhao, *Proc. Natl. Acad. Sci. USA*, **116**, 10064 (2019).
18. F. Vatansever, W. C. de Melo, P. Avci, D. Vecchio, M. Sadasivam, A. Gupta, R. Chandran, M. Karimi, N. A. Parizotto, R. Yin, G. P. Tegos and M. R. Hamblin, *FEMS Microbiol. Rev.*, **37**, 955 (2013).
19. Q. Hong, H. Sun, M. Chen, S. Zhang and Q. Yu, *PLoS One*, **17**, e0274523 (2022).
20. F. Si, X. Zhang and K. Yuan, *RSC Adv.*, **4**, 5860 (2014).
21. B. Kleineidam, M. Nokhbehsaim, J. Deschner and G. Wahl, *Clin. Oral. Investig.*, **23**, 1941 (2019).
22. P. Bhartiya, K. Masur, D. Shome, N. Kaushik, L. N. Nguyen, N. K. Kaushik and E. H. Choi, *Biology (Basel)*, **10**, 1338 (2021).
23. H. Mahdikia, B. Shokri and K. Majidzadeh-A, *Iran. J. Pharm. Res.*, **20**, 337 (2021).
24. C. M. Lee, Y. I. Jeong, M. S. Kook and B. H. Kim, *Int. J. Mol. Sci.*, **21**, 7646 (2020).
25. H. H. Schmidt, K. Wingler, C. Kleinschnitz and G. Dusting, *Circ. Res.*, **111**, e15 (2012).
26. X. Mao, D. L. Auer, W. Buchalla, K. A. Hiller, T. Maisch, E. Hellwig, A. Al-Ahmad and F. Cieplik, *Antimicrob. Agents Chemother.*, **64**, e00576 (2020).
27. D. Lepelletier, J. Y. Maillard, B. Pozzetto and A. Simon, *Antimicrob. Agents Chemother.*, **64**, e00682 (2020).
28. K. D. Bastendorf, N. Strafela-Bastendorf and A. Lussi, *Monogr. Oral Sci.*, **29**, 105 (2021).
29. W. Johnston, B. T. Rosier, A. Artacho, M. Paterson, K. Piela, C. Delaney, J. L. Brown, G. Ramage, A. Mira and S. Culshaw, *Sci. Rep.*, **11**, 9796 (2021).
30. C. Tomasi, A. Bertelle, E. Dellasega and J. L. Wennström, *J. Clin. Periodontol.*, **33**, 626 (2006).
31. B. F. Gilmore, P. B. Flynn, S. O'Brien, N. Hickok, T. Freeman and P. Bourke, *Trends Biotechnol.*, **36**, 627 (2018).
32. T. T. Gupta and H. Ayan, *Appl. Sci.*, **9**, 3548 (2019).
33. J. Y. Lee, K. H. Kim, S. Y. Park, S. Y. Yoon, G. H. Kim, Y. M. Lee, I. C. Rhyu and Y. J. Seol, *J. Periodontal Implant Sci.*, **49**, 319 (2019).
34. J. Park, J. Lee and C. Choi, *PLoS One*, **6**, 3211 (2011).
35. V. S. S. K. Kondeti, C. Q. Phan, K. Wende, H. Jablonowski, U. Gangal, J. L. Granick, R. C. Hunter and P. J. Bruggeman, *Free Radic. Biol. Med.*, **124**, 275 (2018).
36. H. Xu, R. Ma, Y. Zhu, M. Du, H. Zhang and Z. Jiao, *Sci. Total Environ.*, **703**, 134965 (2020).
37. N. Jha, J. J. Ryu, E. H. Choi and N. K. Kaushik, *Oxid. Med. Cell Longev.*, **2017**, 7542540 (2017).
38. N. Thakur, P. Manna and J. Das, *J. Nanobiotechnol.*, **17**, 84 (2019).
39. H. H. Jang, S. B. Park, J. S. Hong, H. L. Lee, Y. H. Song, J. Kim, Y. H. Jung, C. Kim, D. M. Kim, S. E. Lee, Y. I. Jeong and D. H. Kang, *Nanoscale Res. Lett.*, **14**, 58 (2019).
40. H. L. Su, C. C. Chou, D. J. Hung, S. H. Lin, I. C. Pao, J. H. Lin, F. L. Huang, R. X. Dong and J. J. Lin, *Biomaterials*, **30**, 5979 (2009).
41. S. Bekeschus, A. Kramer and A. Schmidt, *Molecules*, **26**, 5682 (2021).
42. C. Duchesne, N. Frescaline, O. Blaise, J. J. Lataillade, S. Banzet, O. Dussurget and A. Rousseau, *mSphere*, **6**, e0021721 (2021).
43. Y. O. Park, C. M. Lee, M. S. Kim, S. C. Jung, S. W. Yang, M. S. Kook and B. H. Kim, *Jpn. J. Appl. Phys.*, **56**, 01AC01 (2017).
44. E. J. Kim, J. E. Hyun, Y. H. Kang, S. J. Baek and C. Y. Hwang, *Vet. Dermatol.*, **33**, 29-e10 (2021).
45. J. Y. Lee, K. H. Kim, S. Y. Park, S. Y. Yoon, G. H. Kim, Y. M. Lee, I. C. Rhyu and Y. J. Seol, *J. Periodontal. Implant Sci.*, **49**, 319 (2019).

46. A. Privat-Maldonado, A. Schmidt, A. Lin, K. D. Weltmann, K. Wende, A. Bogaerts and S. Bekeschus, *Oxid. Med. Cell Longev.*, **2019**, 9062098 (2019).
47. R. Zhou, R. Zhou, P. Wang, Y. Xian, A. Mai-Prochnow, X. Lu, P. J. Cullen, K. Ostrikov and K. Bazaka, *J. Phys. D Appl. Phys.*, **53**, 303001 (2020).
48. A. L. V. Cubas, F. M. Ferreira, D. B. Gonçalves, M. M. Machado, N. A. Debacher and E. H. S. Moecke, *Chemosphere*, **277**, 130255 (2021).
49. H. Jablonowski, J. Santos Sousa, K. D. Weltmann, K. Wende and S. Reuter, *Sci. Rep.*, **8**, 12195 (2018).
50. O. Lunov, V. Zablotskii, O. Churpita, E. Chánová, E. Syková, A. Dejneka and S. Kubinová, *Sci. Rep.*, **4**, 7129 (2014).
51. L. I. Partecke, K. Evert, J. Haugk, F. Doering, L. Normann, S. Diedrich, F. U. Weiss, M. Evert, N. O. Huebner, C. Guenther, C. D. Heidecke, A. Kramer, R. Bussiahn, K. D. Weltmann, O. Pati, C. Bender and W. Bernstorff, *BMC Cancer*, **12**, 473 (2012).
52. V. Nastasa, A. S. Pasca, R. N. Malancus, A. C. Bostanaru, L. I. Ailincai, E. L. Ursu, A. L. Vasiliu, B. Minea, E. Hnatiuc and M. Mares, *Int. J. Mol. Sci.*, **22**, 11534 (2021).

Supporting Information

The effect of cold atmospheric plasma (CAP) on the formation of reactive oxygen species and treatment of *Porphyromonas gingivalis* biofilm *in vitro* for application in treatment of peri-implantitis

Chang-Min Lee[*,‡], Young-IL Jeong[*,‡], Yun Kyong Lim[**], Joong-Ki Kook[**], Seong-Won Yang[***], Min-Suk Kook[**,†], and Byung-Hoon Kim[*,†]**

*Department of Dental Materials, College of Dentistry, Chosun University, Gwangju 61452, Korea
**Department of Oral Biochemistry, College of Dentistry, Chosun University, Gwangju 61452, Korea
***Department of Ophthalmology, College of Medicine, Chosun University, Gwangju 61452, Korea
****Department of Maxillofacial Surgery, School of Dentistry, Chonnam National University, Gwangju 61186, Korea
(*Received 13 July 2022 • Revised 25 October 2022 • Accepted 6 November 2022*)

MATERIALS AND METHODS

1. Confocal Laser Scanning Microscope

For live/dead staining of bacteria, staining solution was prepared as follows: 1 μL live dye (1 mM) and 1 μL dead dye solution (1 mg/mL propidium iodide) (PI) was added to 1 ml staining buffer. To observe the viability of bacteria, bacteria on the surface of titanium disks was treated with CAP equipment as described above. Then, bacteria on the titanium disks were briefly washed with PBS and then incubated for 10 min with 1 mL of the live/dead cell staining solution at 37 °C. Following this, bacteria on the titanium disks were observed with a confocal laser scanning microscope under dark conditions (Zeiss LSM 800 confocal laser scanning microscope, Carl Zeiss Microscopy, NY, USA).

2. Temperature Measurement for Plasma Jet Flame

Infrared thermographic images of both the plasma jet nozzle and the Ti surface were obtained using a high-resolution infrared thermographic camera (FLIR T335). Temperature data were collected with increasing plasma exposure time and gas flow rate at room temperature with a thermal resolution of ±0.1 °C. Atmospheric temperature and relative humidity were 25 °C and 50%, respectively. The maximum temperature of the APPJ flame was less than 36.5 °C.

3. Contact Angles

The water contact angle on the SLA-treated Ti surface was measured using a contact angle measuring equipment (Model no. GS, Surfacetech, Ansan, Kyunggi-do, Korea). The deionized water (7 μL) was dropped onto the Ti disks and then the water contact angle was automatically measured 4 s later. The software Surfacetech (ver. 1.1.5.6) was used to acquire and interprete images. These experiments were carried out three times independently and expressed as average ±S.D.

RESULTS

As shown in Fig. S1, the peaks of Ar^+, OH and O^- ions observed in the UV range (200 nm-400 nm) and visible range (690 nm-950 nm). Furthermore, OH and O^- ions was also increased when relative volume of oxygen supply was decreased (Fig. S1).

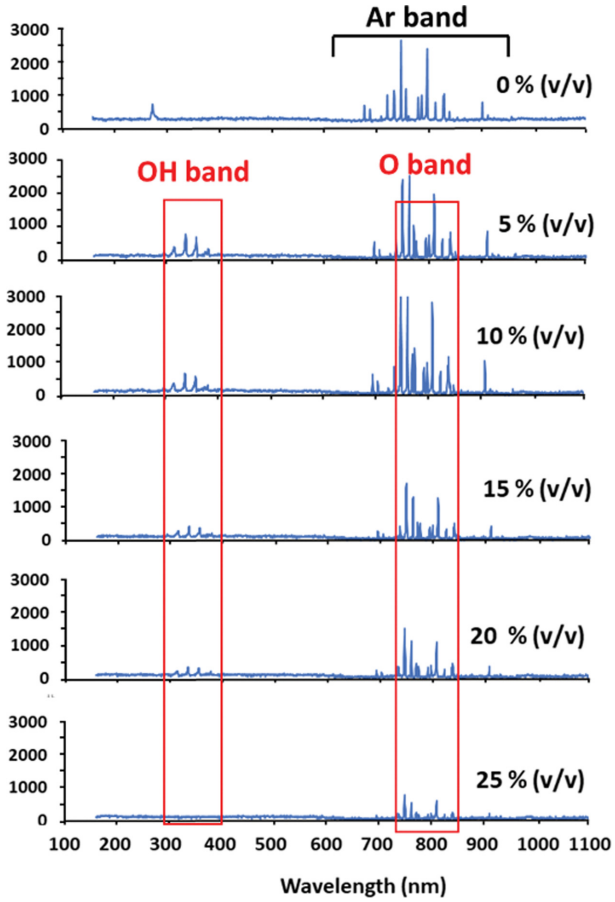

Fig. S1. The effect of volume of oxygen supply on the optical emission spectroscopy (OES) spectrum of CAP plume.

As shown Fig. S2, viable and/or died *P. gingivalis* on the Ti disks were stained with green dye for live bacteria and red dye for died bacteria. When tretament time was increased, died bacteria were relatively increased according to the treatment time.

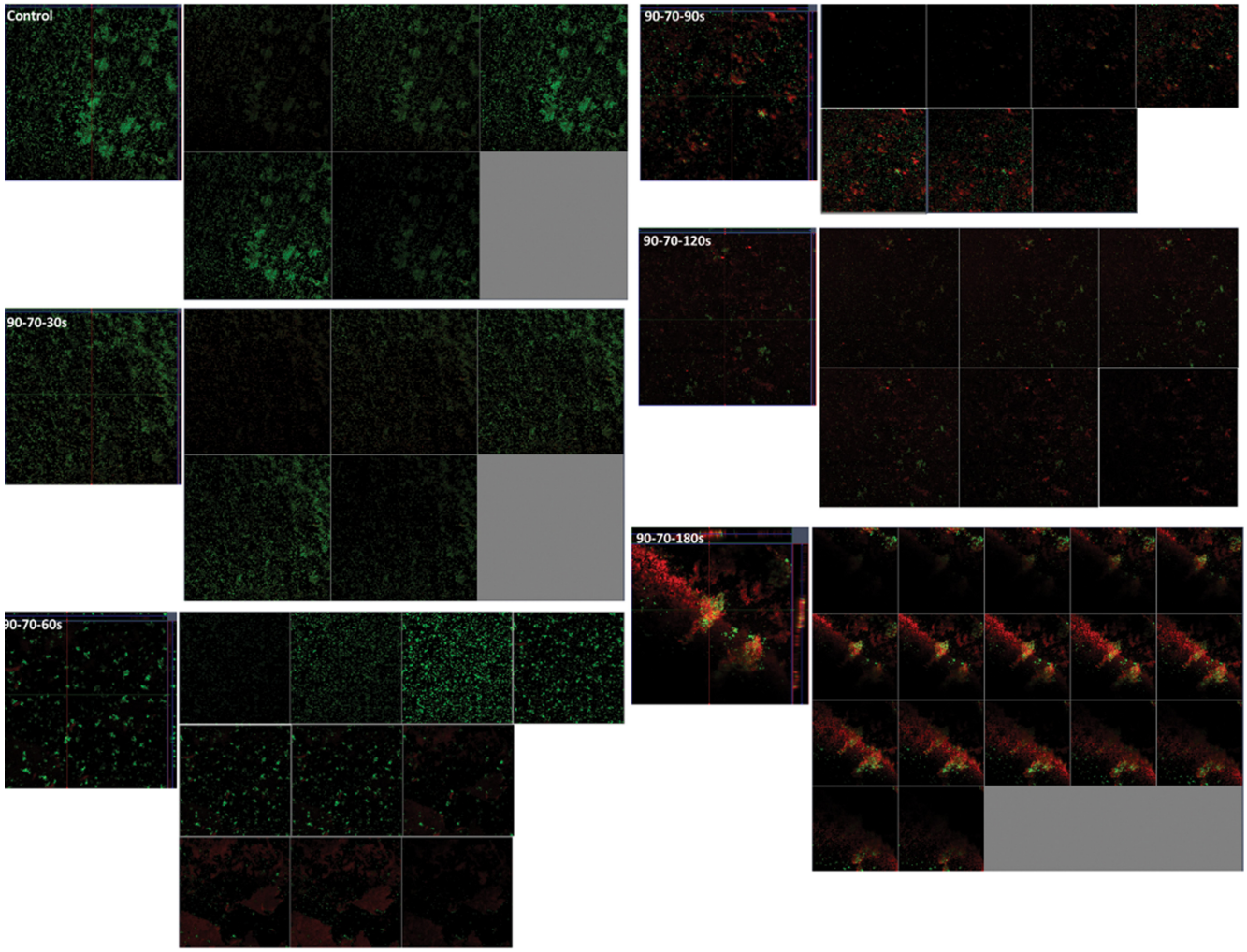

Fig. S2. The effect of treatment time of CAP apparatus on the viability of *P. gingivalis* on the Ti disks. *P. gingivalis* on the Ti disks were treated with CAP apparatus and then stained with live and dead cell dye. Green and red color represents live and dead bacteria, respectively. These figures are raw data of Fig. 7.

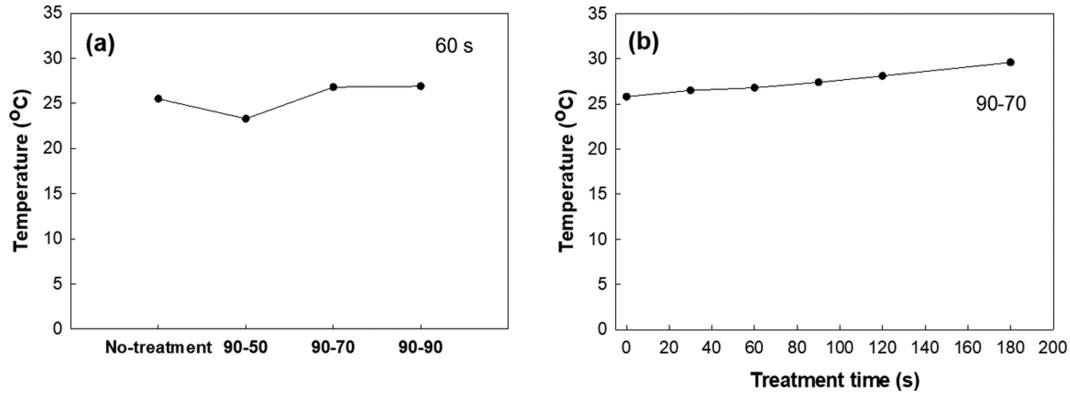

Fig. S3. The changes of temperature of aqueous solution (PBS, 0.01 M, pH 7.4) during CAP treatment.

Fig. S3 shows the effect of CAP treatment on the changes of temperature of aqueous solution. As shown in Fig. S3(a) and (b), temperature of aqueous solution was slightly increased according to the energy level and treatment time. Even though temperature was elevated by CAP treatment, temperature was less than 30 °C at 180 s treatment time. These results indicated that the temperature can be elevated in the area of CAP treatment and then affects to the viability of bacteria or cells in the oral cavity.

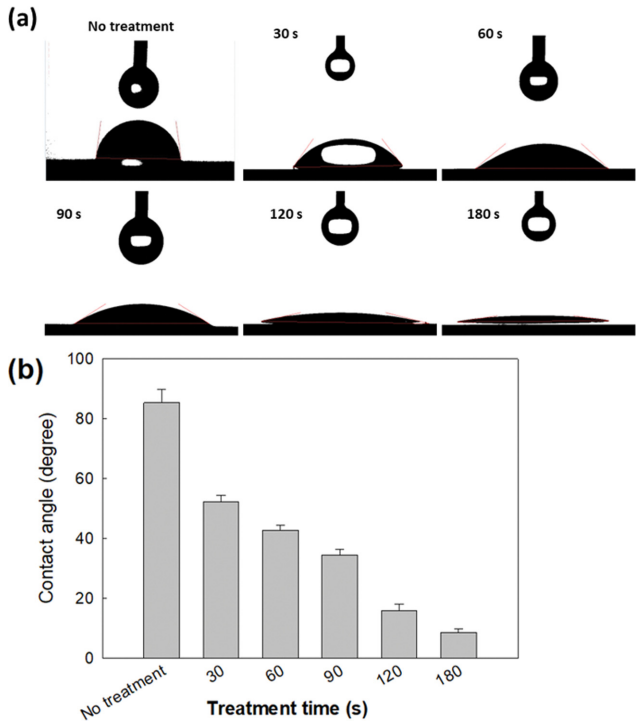

Fig. S4. The effect of CAP-treated time on the Surface wettability of SLA-treated Ti disks. Images of the surface static contact angles of Ti disks were acquired (a) and analyzed quantitatively (b). The indicated values are average±SDs (n=3), No treatment vs. 30, $p<0.01$; No treatment vs. 60, $p<0.01$; No treatment vs. 90, $p<0.01$; No treatment vs. 120, $p<0.01$; No treatment vs. 180, $p<0.01$.

Fig. S4 shows the water contact angle of SLA-treated Ti disks. As swhon in Fig. S4(a) and (b), contact angle was gradually decreased according to the CAP treatment time. These results indicated that CAP treatment affects to the hydrophobic/hydrophilic properties of Ti disks.